

New experimental measurements of the $^{16}\text{O}(p,\alpha)^{13}\text{N}$ reaction rate and its impact on SNIa models

May Alruwaili

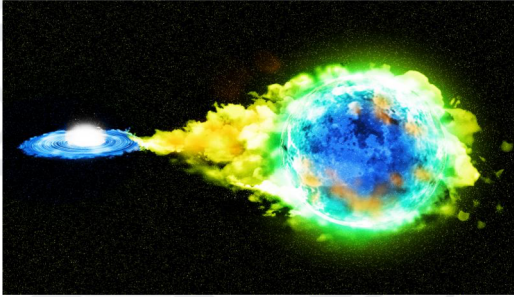
Ph.D student

Nuclear-astrophysics

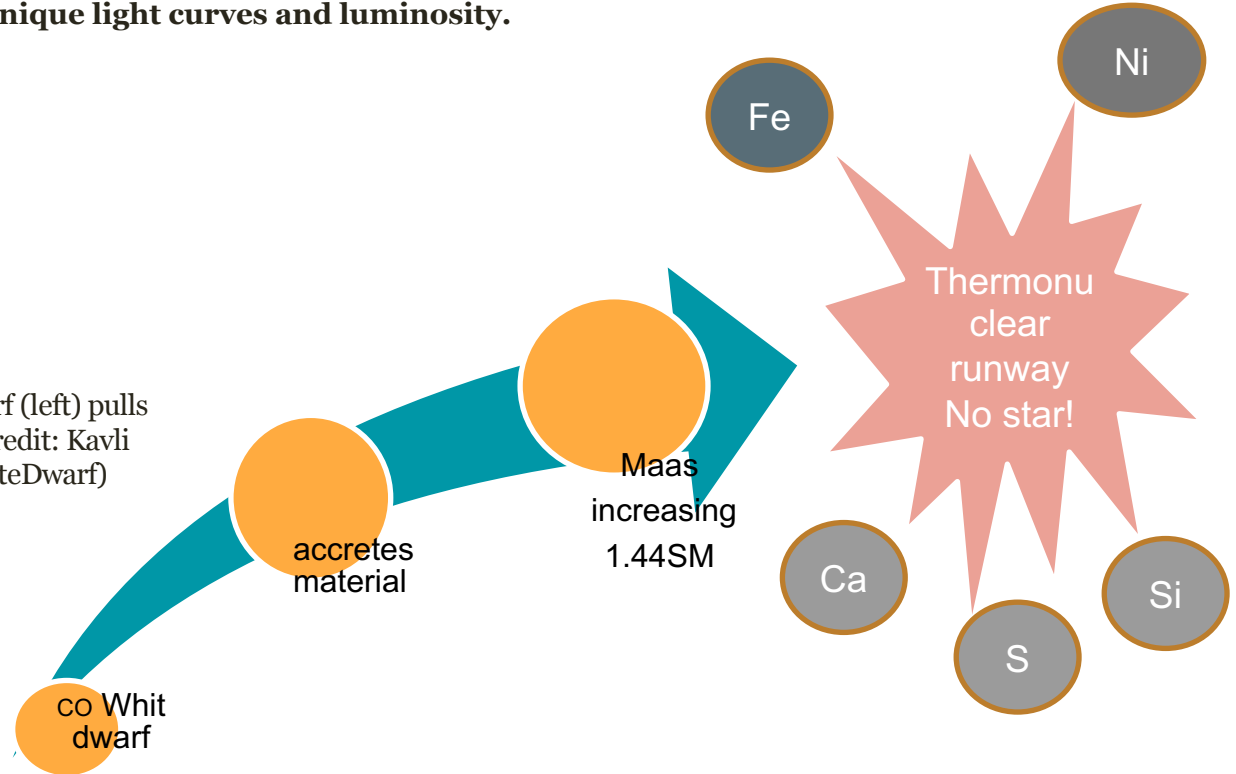
Prof. Alison Laird

Introduction: SNIa explosion Brife

(SNIa), are known cosmic candles.
due to unique light curves and luminosity.



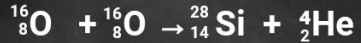
An illustration of a Type Ia supernova, a white dwarf (left) pulls material from a nearby companion star(right). (Credit: Kavli IPMU:<https://www.ipmu.jp/en/20180921-WhiteDwarf>)



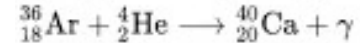
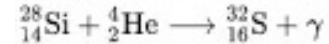
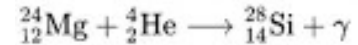
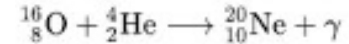
Intermediate mass elements nucleosynthesis in SNIa



Oxygen Burning



Adding alpha particles lead to more heavier elements like (${}^{40}\text{Ca}$, ${}^{32}\text{S}$, Ar ...) to be created. \longrightarrow



Studies have shown how the oxygen burning nucleosyntheses differ with alpha:

- lower alpha lead to more sulfur (${}^{32}\text{S}$) production relative to calcium (${}^{40}\text{Ca}$).
- Higher alpha lead to more calcium (${}^{40}\text{Ca}$) production relative to sulfur (${}^{32}\text{S}$).

$$M_{\text{Ca}}/M_{\text{S}} \propto X_{\alpha}^2$$

(De et al. 2014)



The role of $^{16}\text{O}(p,\alpha)^{13}\text{N}$ in nucleosynthesis of SNIa

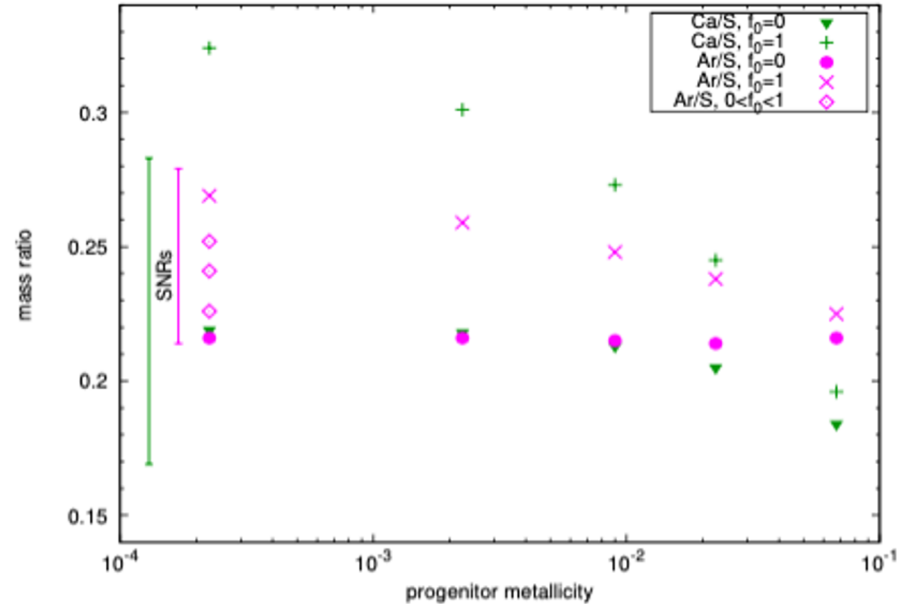


enhances the alpha, boost the $^{12}\text{C}+^{12}\text{C}$ reaction
 → building more of intermediate-mass elements..

$^{16}\text{O}(p,\alpha)^{13}\text{N}$ reaction rate depends on the proton abundance.

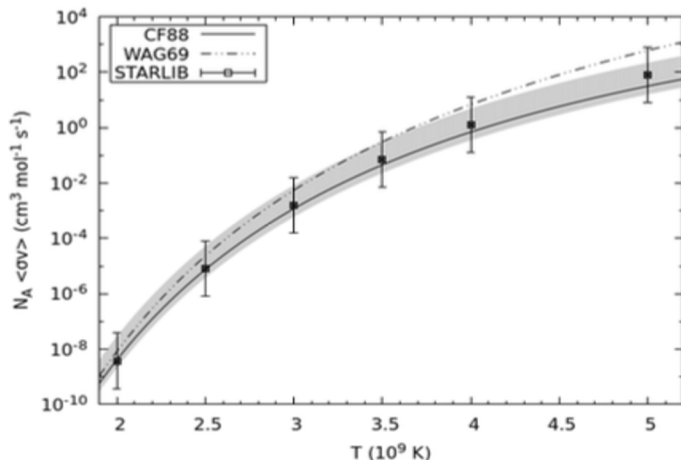
High proton available in lower metallicity progenitor!!

!->increasing Ca/S ratio related to decreasing metallicity and vice versa



Theoretical mass ratios of calcium to sulfur (in green) and argon to sulfur (in magenta) from models of detonation of a $1.06 M_{\odot}$ WD, as function of the progenitor metallicity, with either the standard $^{16}\text{O}(p,\alpha)^{13}\text{N}$ reaction rate ($f_0 = 1$) or the rate switched off ($f_0 = 0$). The argon-to-sulfur mass ratio for $Z = 2.25 \times 10^{-4}$ is shown as well for several other values of f_0 , from bottom to top: $f_0 = 0.1, 0.3,$ and 0.5 . The vertical bars on the left of the figure show the range of observational mass ratios derived from measurements of X-ray emission of SNRs (Martínez-Rodríguez et al. 2017).

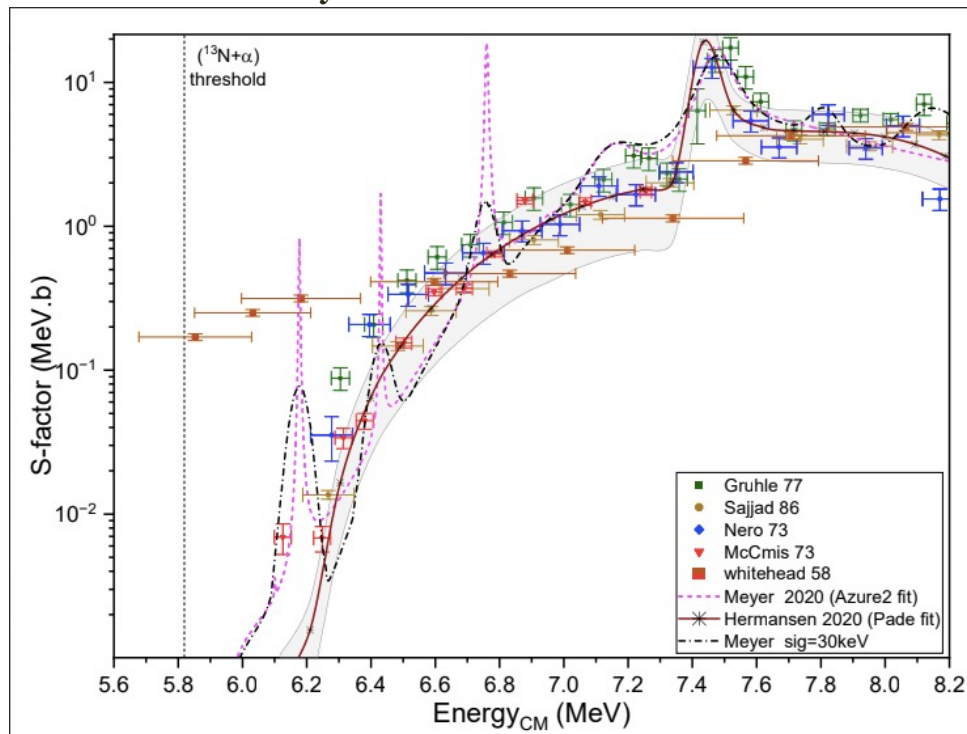
Problem of current $^{16}\text{O}(p,\alpha)^{13}\text{N}$ reaction rates



Rate of the reaction $^{16}\text{O}(p,\alpha)^{13}\text{N}$, as a function of temperature in units of 10^9 K, from different compilations: [Caughlan & Fowler \(1988, CF88\)](#), [Wagoner \(1969, WAG69\)](#), and [Sallaska et al. \(2013, STARLIB\)](#). The uncertainty listed in the STARLIB compilation is plotted as a vertical error bar. The shaded band shows the uncertainty on the rate as determined using measured calcium-to-sulfur and argon-to-sulfur mass ratios in SNRs (see text for details).

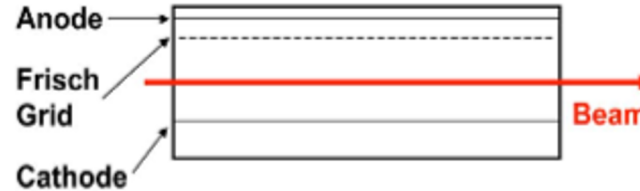
WAG69: no origin
REACLIB: no uncertainty
STARLIB: statistical model

Previous measurements of $^{16}\text{O}(p,\alpha)^{13}\text{N}$ cross-section showed discrepancies on their value, and don't agree within uncertainty.

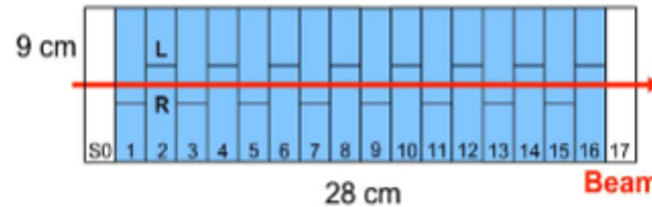


A new measurement of $^{16}\text{O}(p,\alpha)^{13}\text{N}$ Cross-section Ecm = 5.8-6.9 MeV using MUSIC

MUSIC



Schematic of the anode structure



Schematic of the MUSIC detector (from Ref. [5]). Upper panel: lateral view of the detector. Lower panel: anode structure, showing the 18 strips. Strips 1–16 are subdivided into non-symmetric left and right sections.

3

- Each ion travels in the detector loses energy in increments across these strips.
- Each particle has its own pattern in losing Energy
- Eloss (ΔE) $\propto Z$

active target

Gas:
detector & target

All particles
detected

array of 18
anode

Filtering
background

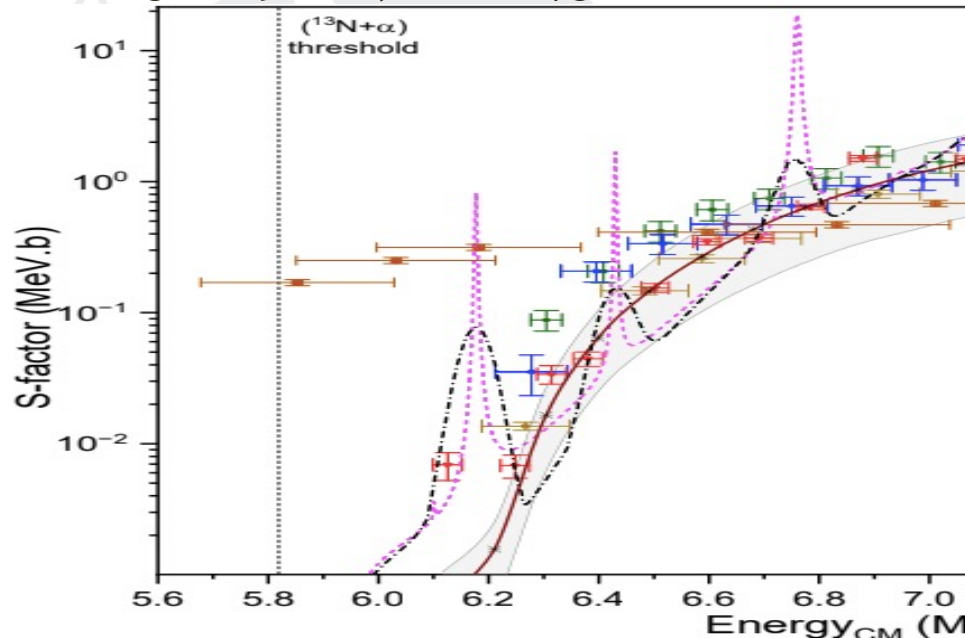
Single Beam
wide Ecm range

MUSIC experimental setup for $^{16}\text{O}(p,\alpha)^{13}\text{N}$



UNIVERSITY
of York

- Inverse kinematics
- 136-MeV ^{16}O beam Energy
- pure methane gas at 700Torr.
- Covers a centre of mass energy range of ~5.8-6.9 MeV, with a 275-keV resolution.



- methane pressure 716,88 (GHS calibration)
- error from strip width (15.8 cm)

Results

Strip	Ecm (MeV)	Error (MeV)
1	6.91231	0.133371
2	6.64159	0.137352
3	6.36252	0.141721
4	6.07425	0.146548
5	5.77578	0.151917
6	5.46593	0.157939
7	5.14323	0.16476
8	4.8059	0.172572
9	4.45168	0.181643
10	4.07768	0.192353
11	3.68006	0.205267
12	3.25353	0.221264
13	2.79045	0.241818
14	2.27897	0.269664
15	1.69854	0.310762
16	1.00705	0.380732

Beam Normalization and events Categorizing:

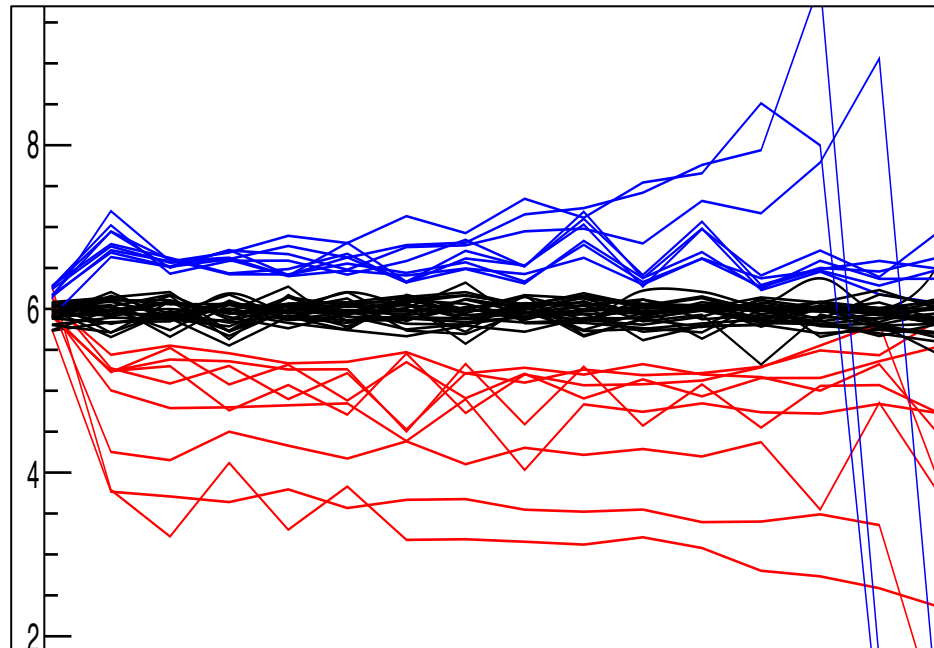


1- background events: excluded.

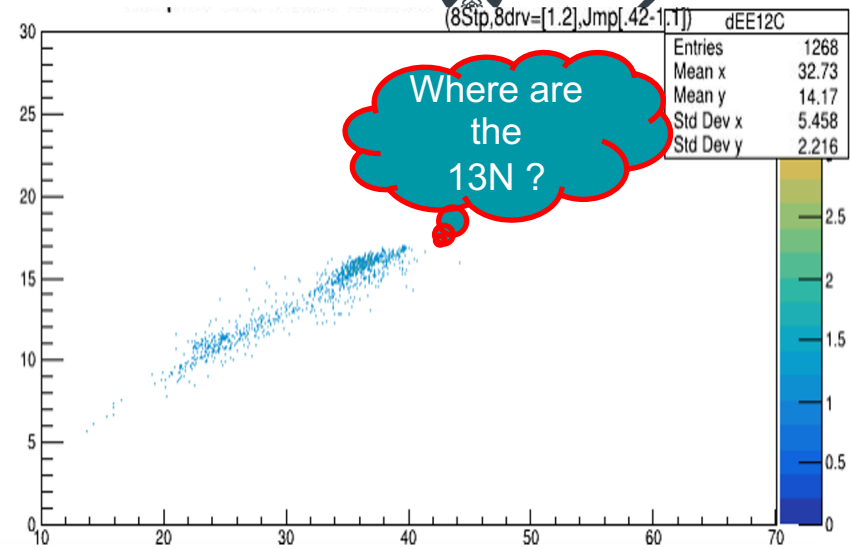
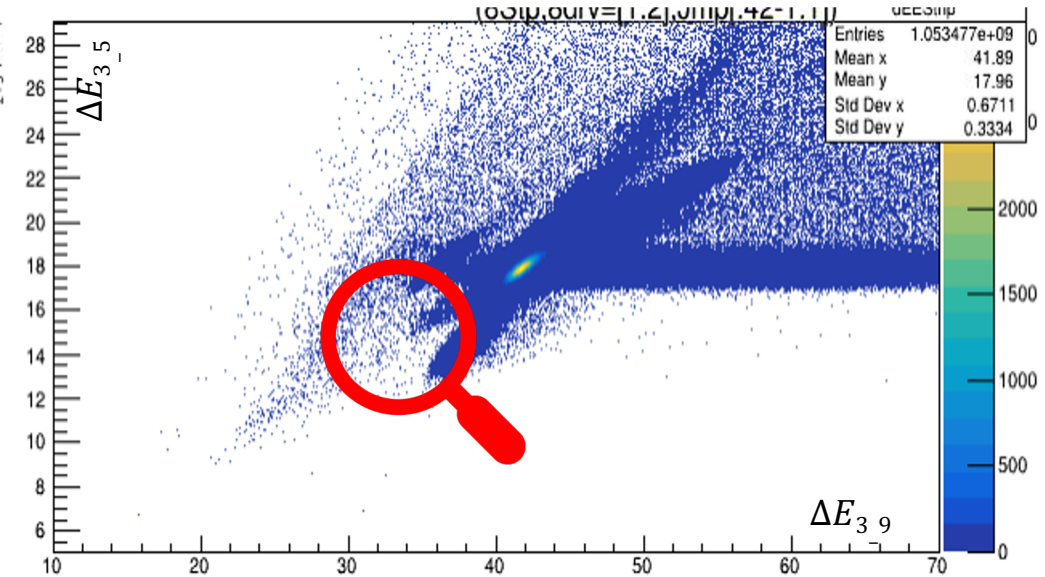
2-Beam events: Normalized Eloss= 6 ± 0.147

3-Jumps on the Eloss:

- Higher events: event with $E_{loss} > 6 + 2(0.147) \rightarrow$ resulted from Ions heavier than beam (potentially ^{25}Mg , ^{26}Al ...).
- Lower events: event with $E_{loss} < 6 - 2(0.147) \rightarrow$ resulted from Ions Lighter than beam (potentially ^{13}N , ^{11}B , ^{12}C ...).



Strip analysis and events counting

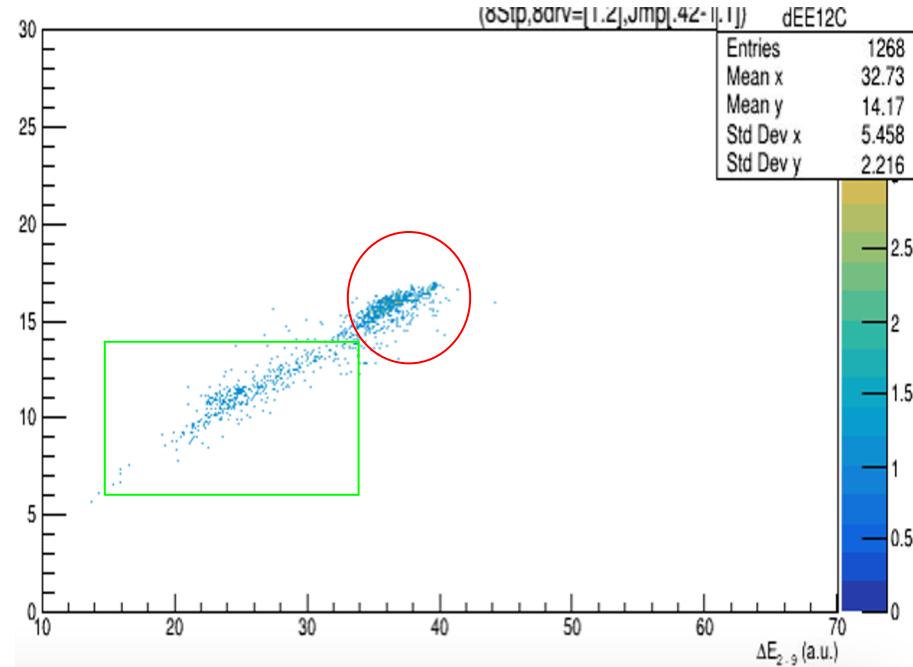
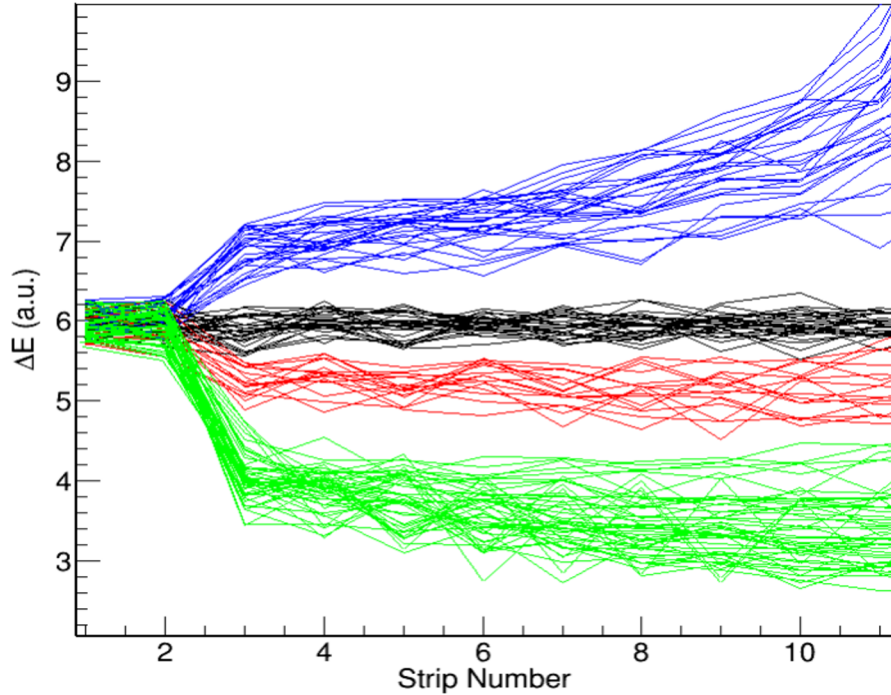


Strip3 unfiltered events (left) compared to the events with Eloss-Only- Lower than the beam (right)

Traces and dE-dE identification

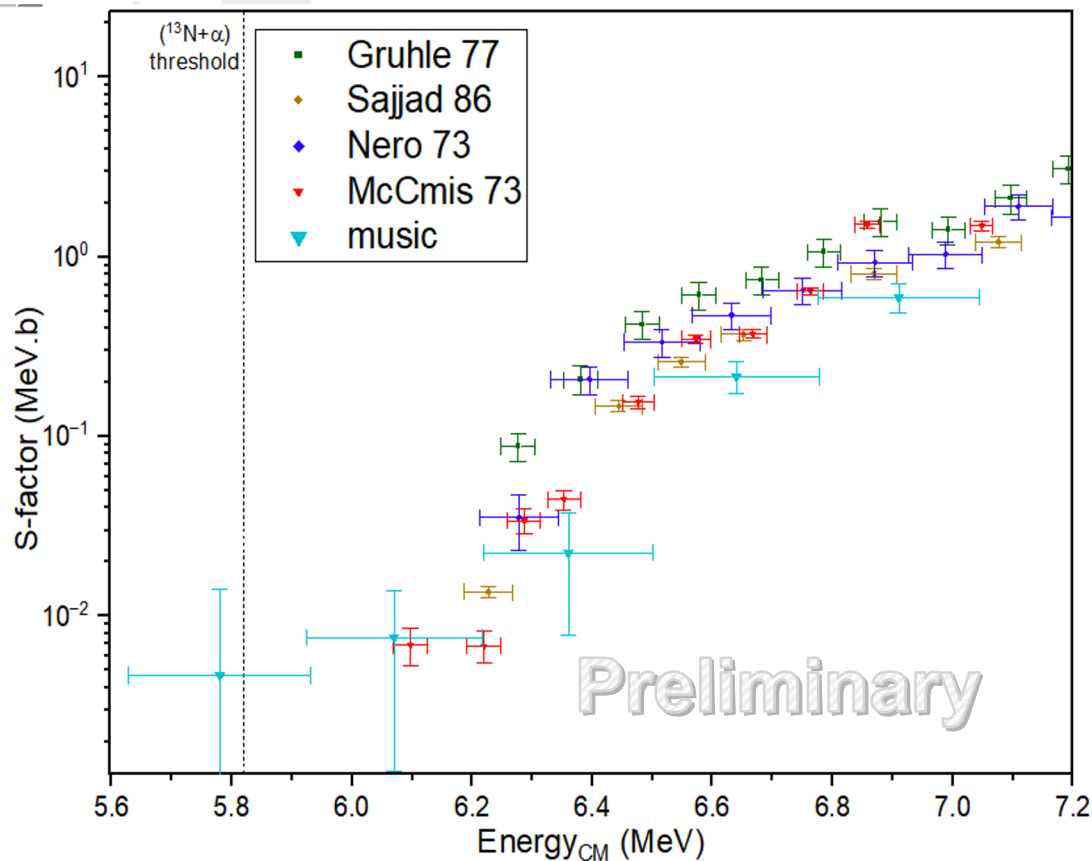


UNIVERSITY
of York



Strip 2 traces compared to the dEE plot shows how the blob in red consistency with the red lined in the traces.. And for the green traces, the scatter of the events is reflected on the green traces .

Cross-section calculation



Summary

- ❖ *The $^{16}\text{O}(p,\alpha)^{13}\text{N}$ reaction can give hints on the metallicity of the SNIa progenitor.*
- ❖ *Previous rates poorly constrained.*
- ❖ *The New cross section measurement with MUSIC provides promises to refine our models of SNIa with reliable rate and meaningful uncertainty.*
- ❖ *Calculating the new rate, after refining the data.*
- ❖ *Helps bridging the gap between theory and observational data have a deeper understanding of SNIa synthesis and progenitor.*



Thanks



UNIVERSITY
of York

A. Laird¹, H. Jayatissa², N. de Séréville³,
M. Avila², C. Fougères³, B. Kay², S. Chakraborty¹,
C. Barton¹, C. Diget¹, A. Hall-Smith¹, W. Ong⁴, E. Rehm².

N. DE. SÉRÉVILLE,² E. BRAVO,³ C. DIGET,¹ R. LONGLAND,^{4,5} AND C. BADENES³

² Physics Division, Argonne National Laboratory, Lemont, IL 60439, USA

³ Institut de Physique Nucléaire d'Orsay (IPNO), CNRS/IN2P3 et Université Paris-Sud,
91405 Orsay, France

⁴ Lawrence Livermore National Laboratory, 7000 East Ave, Livermore, CA 94550, USA

⁴ *Department of Physics North Carolina State University, Raleigh, North Carolina 27695-8202, USA*

⁵ *Triangle Universities Nuclear Laboratory, Durham, North Carolina, 27708-0308, USA*